Cancer Research

Gender-Specific Molecular and Clinical Features Underlie Malignant Pleural Mesothelioma

Assunta De Rienzo[1], Michael A. Archer[1], Beow Y. Yeap[2], Nhien Dao[1], Daniele Sciaranghella[1], Antonios C. Sideris[1], Yifan Zheng[1], Alexander G. Holman[3], Yaoyu E. Wang[3], Paola S. Dal Cin[4], Jonathan A. Fletcher[4], Renee Rubio[3], Larry Croft[5], John Quackenbush[3], Peter E. Sugarbaker[1], Kiara J. Munir[1], Jesse R. Battilana[1], Corinne E. Gustafson[1], Lucian R. Chirieac[4], Soo Meng Ching[5], James Wong[5], Liang Chung Tay[5], Stephen Rudd[5], Robert Hercus[5], David J. Sugarbaker[6], William G. Richards[1], and Raphael Bueno[1]

Abstract

Malignant pleural mesothelioma (MPM) is an aggressive cancer that occurs more frequently in men, but is associated with longer survival in women. Insight into the survival advantage of female patients may advance the molecular understanding of MPM and identify therapeutic interventions that will improve the prognosis for all MPM patients. In this study, we performed whole-genome sequencing of tumor specimens from 10 MPM patients and matched control samples to identify potential driver mutations underlying MPM. We identified molecular differences associated with gender and histology. Specifically, single-nucleotide variants of *BAP1* were observed in 21% of cases, with lower mutation rates observed in sarcomatoid MPM ($P < 0.001$). Chromosome 22q loss was more frequently associated with the epithelioid than that nonepithelioid histology ($P = 0.037$), whereas *CDKN2A* deletions occurred more frequently in nonepithelioid subtypes among men ($P = 0.021$) and were correlated with shorter overall survival for the entire cohort ($P = 0.002$) and for men ($P = 0.012$). Furthermore, women were more likely to harbor *TP53* mutations ($P = 0.004$). Novel mutations were found in genes associated with the integrin-linked kinase pathway, including *MYH9* and *RHOA*. Moreover, expression levels of *BAP1*, *MYH9*, and *RHOA* were significantly higher in nonepithelioid tumors, and were associated with significant reduction in survival of the entire cohort and across gender subgroups. Collectively, our findings indicate that diverse mechanisms highly related to gender and histology appear to drive MPM. *Cancer Res; 76(2); 319–28. ©2015 AACR.*

Introduction

Malignant pleural mesothelioma (MPM) is a rare, aggressive cancer, associated with prior exposure to asbestos (1). Approximately 3,200 new cases are diagnosed in United States annually, and the incidence worldwide is estimated to rise during the next two decades (2). Prognosis is poor for most patients with a reported median survival between 4 and 12 months because there are few effective systemic treatments for this malignancy (3). Three major histologic types are recognized in MPM: epithelioid, sarcomatoid, and biphasic (4). The incidence of MPM is higher in men than women, likely because of the more common occupational asbestos exposure in men, whereas women are usually subject to secondary exposure through spouses' clothing, low-level environmental exposure, and other sources (5, 6). A recent study suggests that female patients with MPM live significantly longer compared with men even after adjustment for potential confounders such as age, stage, and treatment (5).

High-throughput sequencing techniques have revealed that each cancer genome appears to have a unique genetic profile acquired through cumulative genetic alterations, including driver mutations, that may confer advantageous survival phenotypes on the cancerous cells and represent precise therapeutic targets (7). To date, the genetic landscape of MPM has been primarily described in terms of chromosomal rearrangement events investigated mostly in epithelioid and biphasic human specimens and cell lines (8). The cyclin-dependent kinase inhibitor 2A (*CDKN2A*), the neurofibromatosis type 2 (*NF2*), and the BRCA1-associated protein-1 (*BAP1*) genes have been shown to be the most frequently mutated tumor suppressor genes in MPM (9–12). Recently, two independent investigations have identified *BAP1* as frequently mutated in the chromosomal region 3p21.1 in sporadic and familial MPM, indicating the importance of genetic factors in MPM susceptibility (10, 12, 13). Although *BAP1*

[1]The Thoracic Surgery Oncology laboratory and the International Mesothelioma Program, Division of Thoracic Surgery and the Lung Center, Brigham and Women's Hospital, and Harvard Medical School, Boston, Massachusetts. [2]Department of Medicine, Massachusetts General Hospital and Harvard Medical School, Boston, Massachusetts. [3]Center for Cancer Computational Biology, Department of Biostatistics and Computational Biology, Dana-Farber Cancer Institute, and Harvard School of Public Health, Boston, Massachusetts. [4]Departments of Pathology, Brigham and Women's Hospital, and Harvard Medical School, Boston, Massachusetts. [5]Malaysian Genomics Resource Centre, Kuala Lumpur, Malaysia. [6]Debakey Department of Surgery, Baylor College of Medicine, Houston, Texas.

Note: Supplementary data for this article are available at Cancer Research Online (http://cancerres.aacrjournals.org/).

M.A. Archer and B.Y. Yeap contributed equally to this article.

Corresponding Author: Assunta De Rienzo, Division of Thoracic Surgery, Brigham and Women's Hospital 75 Francis Street, Boston, MA 02115. Phone: (617) 732-6526; Fax: (617) 566-3441; E-mail: aderienzo@partners.org.

doi: 10.1158/0008-5472.CAN-15-0751

mutations have been associated with age (10) and with the epithelioid subtype (14), no other significant correlation of these genes to demographic, clinical, or pathologic variables has so far been identified.

In the current study, a comprehensive genome-wide approach was applied to discover novel genetic alterations in MPM. Whole-genome sequencing data of tumor specimens from 10 MPM patients and their matched normal tissue were analyzed to identify novel somatic point mutations. A bioinformatic approach was employed to prioritize genes to further analyze by focused sequencing in close to three hundred additional MPM tumor samples.

Materials and Methods

Specimens and cell lines

All tumor and normal lung specimens were collected at surgery with patient consent, freshly frozen, stored, and annotated by the institutional tumor bank with Institutional Review Board approval at Brigham and Women's Hospital (BWH; Boston, MA). High quality, tumor enriched (15) samples were prepared as previously described (16). Tumor cell enrichment (>83% for whole-genome sequencing experiments; >40% for targeted resequencing experiments) was confirmed by reviewing hematoxylin and eosin (H&E)-stained frozen sections. Eleven mesothelioma cell lines (H2052, MSTO-211H, H2452, H28, and the epithelial virus transformed MET5A from the (ATCC), JMN and JMN1B from Cell Culture Core (BWH), and MESO257, MESO428, MESO589, MS924 from the laboratory of J.A. Fletcher] were cultured in RPMI (Invitrogen Corporation) containing 10% FBS (ATCC) and maintained at 37°C in 5% CO_2. Cells were collected at 70% confluence and frozen for DNA extraction or placed in RNA extraction buffer (TRIzol reagent, Invitrogen) for RNA extraction. DNA was isolated using the DNeasy Tissue Kit (Qiagen) and RNA using the TRIzol (Thermo Fisher) method in combination with RNeasy kit (Qiagen). RNase or DNase I (Qiagen) treatments were conducted according to the manufacturer's instructions. Matched normal DNA was prepared from peripheral blood or lung tissue. Nucleic acids were quantified using an ND-1000 spectrophotometer (Thermo Fisher). The integrity of the DNA and RNA were determined using Qubit 2.0 Fluorometer (Thermo Fisher) and Agilent 2100 Bioanalyzer (Agilent), respectively.

Whole-genome sequencing

Whole-genome sequencing of 10 tumor and 10 matched normal genomic DNA (obtained from blood) samples (3 μg) was accomplished using a Complete Genomics platform (17). Mean coverage of tumor and normal genomes were 187× and 188×, respectively (Supplementary Table S1). All the pair-end reads were filtered on the basis of average read quality score ≥ 20. Candidate somatic mutations were detected using the SynaAlign program (Synamatix). Briefly, sequencing reads were first aligned to the human reference genome (hg19) using short read mapper SXmapper (Synamatix) with default parameter settings. The numbers of reads containing single nucleotide variants (SNV) and indels in both tumor and germline samples were counted and the quality score of each base and the read direction information were collected. This information and the mapping statistics for each read across the genome (reads in repeat regions etc.) were used to call SNVs and indels. The null hypothesis of equal allele frequencies in tumor and germline samples was tested using the two-tailed Fisher exact test on quality-filtered SNVs and indels. Data were also collected for each sample on larger scale structural variations, loss of heterozygosity, and copy number variations.

Validation of SNV by Sanger sequencing

Selected candidate SNVs were further characterized using PCR and conventional Sanger sequencing to confirm tumor-specific single-nucleotide mutations. Gene-specific primer pairs were used to PCR amplify genomic DNA from tumor and normal specimens (Supplementary Table S2) as previously described (16). For TP53 analysis, primers were chosen in the flanking intronic region of each exon. Twenty-two samples were analyzed using both resequencing and Sanger methods. Discordant results were found in six cases, probably due to tissue heterogeneity. In discordant cases, the mutation was called as present for each sample.

Karyotype and FISH analysis

Metaphase chromosome spreads from diagnostic MPM samples were prepared and G-banded according to standard procedures as part of the routine BWH pathologic evaluation of all MPM cases. Additional FISH analyses were performed in those samples either with no metaphases or normal karyotype in the context of pathologic mesothelioma positive report. FISH analysis was performed using the Vysis LSICDKN2A/CEP9 Dual Color Probe Set (Abbott Molecular) for the *CDKN2A* locus at 9p21, CEP9 at the chromosome 9 centromeric region, and Vysis TUPLE 1/LSI ARSA Dual Color Probe Set (Abbott) for TUPLE 1 at 22q11.2 and ARSA at 22q13. Observed aberration in $\geq$ 2% of observed nuclei (minimum 50 per case) was reported as consistent with a clonal, neoplastic, and cellular proliferation.

Additional dual-color FISH analysis

For a subset of cases, dual-color FISH analysis was performed on frozen sections (5 μm) to assess two distinct regions of chromosome 22. The sections were fixed at room temperature for two hours in freshly prepared 3:1 methanol:acetic acid, then air-dried.

Bacterial artificial chromosome (BAC) DNA probes (CHORI, BAC PAC Resource) containing most or all of the coding sequence for *NF2* (RP11-155B12, 159 kb) and *MYH9* (RP11-105I18, 161 kb) were selected and labeled by nick translation (Abbott), *NF2* with Orange dUTP, and *MYH9* with Green dUTP. Slides were pretreated with pepsin (Digest-All 3, Invitrogen) 5 to 15 minutes at 37°C, rinsed in PBS for 5 minutes at room temperature, post-fixed 1 minute in 10% formalin, rinsed in PBS, dehydrated in ethanol series, and air-dried. FISH procedure followed standard protocols. Scoring was performed by two technologists, each scoring Orange (O, NF2) and Green (G, MYH9) signals present on 50 nuclei, for 100 nuclei total per specimen in an area determined by a pathologist in parallel H&E-stained sections to have a minimum tumor involvement of 40%. Negative controls were a normal lymphoblast line with metaphases to confirm localization, and sections from four tumors with no histologically apparent tumor in the scored areas. Each deletion signal pattern (1O1G, 1O2G, 2O1G) was determined to be present if its frequency exceeded the mean plus 3 SDs of the same pattern in the normal sections.

Target capture, sequencing, and data analysis

Library preparation, custom exome capture, and next-generation sequencing were performed at the Center for Cancer

Computational Biology. Library construction and custom exome capture were performed using the SureSelect XT2 for Illumina protocol (Agilent) according to the manufacturer's instructions Libraries were combined to 3 library pools, diluted to a 2 nmol/L working stock and sequenced at a final concentration of 12 pmol/L on a paired end flowcell with 50 cycles in each direction. Sequencing was done on a HiSeq 2000 (Illumina) according to the manufacturer's protocols. Sequencing reads were demultiplexed using the Illumina CASAVA package and aligned to the hg19 assembly of the human genome using BWA aln with default parameters and a mismatch penalty of 1 (18). SNV and indel discovery was performed using HaplotypeCaller within the GATK package with default parameters (19). Variants with a minimum phred-scaled confidence threshold under 10 were excluded, and those under 30 were flagged as low quality. Resulting variant calls were annotated for potential genetic impact using the SnpEff package (20).

Microarray analysis

Expression levels of specific genes were explored using microarray data from a parallel project. Epithelioid samples ($N = 129$) were selected from the International Mesothelioma Program Tumor Bank (Supplementary Fig. S1). This sample set consisted of male and female samples matched by age and nodal status (Coleman MH, and Bueno R; personal communication). In addition, 19 sarcomatoid and 3 biphasic MPM samples were included in the analysis. To determine the levels of transcripts in each sample, 0.25 μg of total RNA was amplified using the Ambion WT Expression Kit (Thermo Fisher). The cRNA was hybridized to Affymetrix Human Gene 1.1 ST Array (Thermo Fisher), subsequently labeled with GeneChip WT Terminal Labeling Kit (Thermo Fisher), and scanned with a GeneAtlas Workstation (Thermo Fisher). Hybridization, washing, staining, and scanner procedures were performed per manufacturer's recommendations. For quality control across platforms, two MAQC samples were included in the analysis (21). A blind control was also added to check the variability of the expression values across the chips. The probe intensity distribution was examined for quality control and outliers were removed. Expression levels for *BAP1*, *NF2*, *TP53*, *MYH9*, *MYH6*, *MYH10*, *PIK3C2A*, *RHOA*, and *TNFRSF1A* for this cohort are included in Supplementary Table S3.

Statistical analysis of mutation status and gene expression versus clinicopathologic variables

Asbestos exposure was analyzed as a binary covariate with background exposure defined as asbestos body counts in lung tissue ≤ 50 fibers per gram of wet lung tissue. Fisher exact test was used to compare histology, gender, and asbestos exposure between mutation and wild-type groups, whereas Wilcoxon rank sum test was used to analyze age as a continuous covariate. Overall survival was defined from the date of definitive surgery until the date of death or was censored at the date of last follow-up for patients who had not died at their latest contact. Overall survival was estimated by the Kaplan–Meier method, with group differences assessed by the log-rank test. The normalized expression level of each candidate gene was initially grouped into quartiles for exploratory survival analysis. Patient subgroups with comparable survival were combined for further analysis to estimate the meaningful differences. Proportional hazards regression was used to estimate the HR for reporting a survival difference, including adjusting for the gender effect. All P values are based on a two-sided hypothesis, with $P < 0.01$ used to identify potentially significant results to be conservative on false positives. Data analysis was performed using SAS 9.4 (SAS Institute).

Results

Experimental subjects

Ten MPM tumor and matched normal DNA samples were analyzed by whole-genome sequencing (Table 1). Matched MPM and normal DNA from 283 additional patients was subjected to focused sequencing (Table 2).

Tumor somatic DNA variants

Point mutations, small (<30 bp) structural variations, and copy number alterations were discovered in 10 pairs of whole-genome sequencing MPM tumor and germline DNA samples using computational approaches. Single nucleotide variants (N = 146; SNVs) mapping in the amino acid coding regions of annotated exons and generating nonsynonymous amino acid changes were further resequenced in the tumor and normal DNA by Sanger methodology. Eighty-five were confirmed to be tumor-specific (Supplementary Table S2). Each patient's sample pair displayed a unique small number of point mutations ranging from three to 20 per tumor. Seventy-eight SNVs were missense and seven were nonsense mutations. *TP53* was found mutated in 2 of 10 tumors (20%). In both cases, the tumors came from female patients with asbestos body counts in the background range as measured in resected lung tissue (data not shown). Three of the mutated genes (*RNF43*, *TP53* and *MYH9*) were listed in the Catalogue Of Somatic Mutation In Cancer (COSMIC, Release v69) database (22).

Table 1. Clinical and molecular characteristics of the 10 MPM samples included in the whole-genome sequencing analysis

Tumor sample	Histology	Gender	Asbestos body counts	9p (FISH)	22q (FISH)
CG3	Biphasic	M	N/A	N/A	N/A
CG5	Biphasic	M	87	Abnormal	Abnormal
CG4	Epithelial	M	25	Abnormal	N/A
CG10	Biphasic	M	N/A	Normal	Normal
CG9	Epithelial	M	934	Normal	Abnormal
CG12	Biphasic	M	1,382	Normal	Abnormal
CG14	Epithelial	F	6	Abnormal	Abnormal
CG16	Epithelial	F	3	Abnormal	Abnormal
CG18	Epithelial	F	0	Normal	N/A
CG20	Epithelial	M	25	Normal	Abnormal

Abbreviation: N/A, not available.

Table 2. Clinical and histopathologic characteristics of patients in mutational and expression analyses

	Mutational	Expression
Evaluable for analysis	283	151
Alive at last follow-up	34 (12%)	6 (4%)
Follow-up from surgery, months		
Median (range)	45 (2–106)	59 (4–99)
Age, years		
Median (range)	61 (17–84)	59 (17–75)
Gender		
Male	195 (69%)	85 (56%)
Female	88 (31%)	66 (44%)
Histologic subtype		
Epithelioid	205 (72%)	129 (85%)
Biphasic	52 (18%)	3 (2%)
Sarcomatoid	25 (9%)	19 (13%)
Desmoplastic	1 (<1%)	0
Asbestos body counts per gram wet lung tissue[a]		
≤50 fibers	67 (45%)	31 (37%)
>50 fibers	81 (55%)	53 (63%)

[a]Asbestos data missing for 135 patients in mutational analysis and for 67 patients in expression analysis.

Functional analysis of point mutations

To identify clusters of genes associated with known pathways, functional enrichments of genes affected by point mutations were performed utilizing Ingenuity Pathway Analysis (Qiagen) using Biological Process Gene Ontology terms and canonical pathways. Among 216 canonical pathways identified, 51 were significantly enriched ($P < 0.05$) for the mutated genes (Supplementary Table S4). Mutations affecting genes involved in the integrin-linked kinase (ILK) pathway were the most significantly ($P = 4.9e{-}5$) enriched. Specifically, 5 of the 10 sequenced MPM samples showed point mutations in at least one of 6 identified genes associated with this pathway (*MYH9*, *MYH6*, *MYH10*, *PIK3C2A*, *RHOA*, and *TNFRSF1A*; Fig. 1A).

Validation of the candidate driver genes in an independent cohort

To further assess the prevalence of mutations observed herein and in previous studies (9–12), a panel of 147 MPM tumors (including 81 epithelioid, 41 biphasic, 24 sarcomatoid, and 1 desmoplastic) and 11 previously established MPM cell lines were further analyzed using targeted resequencing of *BAP1*, *NF2*, *TP53*, *MYH9*, *MYH6*, *MYH10*, *PIK3C2A*, *RHOA*, and *TNFRSF1A*. This cohort included tumor samples from women ($n = 30$) to evaluate the frequency of mutations with respect to gender. In addition, clinical karyotype analysis and FISH data for *CDKN2A* and 22q were available for most of the patients. Targeted resequencing revealed 116 nonsynonymous SNVs and/or INDELs (Supplementary Table S5A–S5C). Seven of these were confirmed to be single-nucleotide polymorphisms occurring at high frequency (>1%–2%) in the normal population. The remaining 109 occurring in 86 samples were further examined in normal and tumor DNA pairs by Sanger sequencing. One or more somatic mutations were confirmed in 81 of 147 samples (55%).

BAP1 was mutated in 31 of 147 (21%) samples (Supplementary Table S5A). Twenty-six tumor-specific variants and 5 germline variants (present in tumor and normal matching DNA) were observed. In six samples, multiple *BAP1* mutations were identified. The mutations occurred mostly in epithelioid (23%) and biphasic (24%) samples, whereas only two of 24 sarcomatoid (8%) samples had tumor-specific *BAP1* mutations. No significant correlation was found between mutation in *BAP1* and gender, exposure to asbestos, or survival. *BAP1* mutations were associated with marginally older age compared with wild-type tumors (median 67 vs. 64 years; $P = 0.050$). *BAP1* mutations were also observed in cell lines H2452 and H28. Table 3 describes the cases carrying *BAP1* germline mutations.

NF2 point mutations occurred in 21 (14%) of 147 analyzed samples (Supplementary Table S5A). In addition, karyotype, and/or FISH analyses available for 133 of these 147 samples showed that 75 samples (56%) had loss of chromosome 22q. Eleven of 133 (8%) had both *NF2* point mutation and 22q deletion. Compared with the cases with two copies of 22q, the deletion of 22q was more frequently associated with the epithelioid than nonepithelioid histology ($P = 0.037$). The difference was greater in women but did not reach strict statistical significance due to low power ($P = 0.141$). Mutations in *NF2* were not correlated with any of the other clinical or pathologic variables examined. *NF2* mutation was found in H2052.

Karyotyping and/or FISH analyses of *CDKN2A* were available for 133 of 147 samples. Eighty-two (62%) of 133 samples had deletion of the *CDKN2A* region on 9p (determined by karyotyping) and/or confirmed *CDKN2A* deletion (as determined by FISH with a *CDKN2A* probe). Forty-one of 74 (55%) epithelioid, 29 of 41 (71%) biphasic, 11 of 17 (65%) sarcomatoid, and one of one desmoplastic samples had *CDKN2A* deletion. Compared with the cases with two copies of *CDKN2A*, cases with CDKN2A deletion appeared to be more frequently associated with the nonepithelioid histology ($P = 0.117$). When this analysis was repeated for gender, the association between histology and *CDKN2A* loss was statistically significant only for the men ($P = 0.021$). Interestingly, deletions in CDKN2A were correlated with shorter overall survival in the whole cohort ($P = 0.002$), but the difference was statistically significant only in the men ($P = 0.012$).

TP53 was mutated in 22 cases (15%) in this sample set (Supplementary Table S5B). Three mutations (D49N, C176F, A86T) were present in both the tumor and the normal DNA (Table 3). Notably, one sample showed only one germline *TP53* mutation (D49N) and no mutation in any of the other genes investigated herein. None of the cell lines examined exhibited TP53 mutations.

No difference was observed in overall survival between the group of 62 patients with point mutation in at least one of the established MPM-related genes (*BAP1*, *NF2*, *TP53*) and the group wild-type for these genes ($P = 0.646$).

Forty SNVs in 31 samples (21%) occurred in ILK pathway–associated genes (*TNFRSF1A*, *PIK3C2A*, *MYH10*, *MYH6*, *MYH9*, and *RHOA*; Supplementary Table S5C), of which 35 (88%) were germline. Fifteen patients (43%) carrying a germline mutation in one or more of these genes had familial history of cancer. Only one SNV, in *TNFRSF1A*, is known to occur frequently (>1%–2%) in the general population (23). This SNV occurred in 5 patients and was predicted to have a "probably damaging" effect (PolyPhen: http://genetics.bwh.harvard.edu/pph2/) on the corresponding protein. Seven germline mutations were identified in *PIK3C2A*. Five were predicted to be benign and two "possibly damaging", one of which resides in the PI3K C2 domain. Twenty-six SNVs resided in three myosin heavy chain genes. Two samples displayed germline mutation of *MYH10*. Although functional analyses predict a benign effect, these mutations occur near mutations identified in other cancers (24). Nine germline mutations were detected in *MYH6*, two of which had a predicted

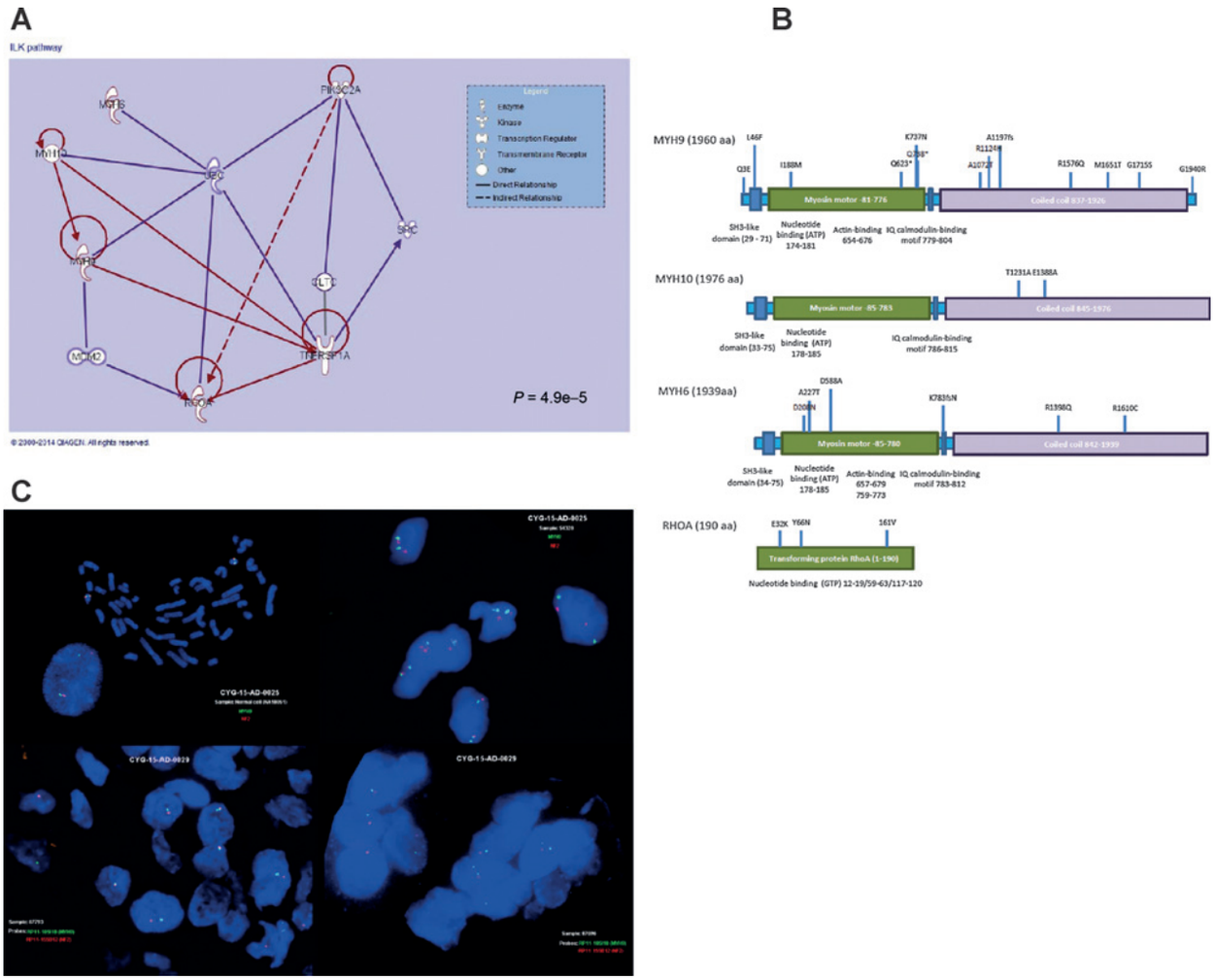

Figure 1.

A, Ingenuity Pathway Analysis was used to connect a subset of six genes (*MYH9, MYH6, MYH10, PIK3C2A, RHOA,* and *TNFRSF1A*), with tumor specific mutations in five MPM samples, mapping in the integrin-linked kinase pathway. Four genes (*UBC*, *MDM2*, *CLTC*, and *SRC*) were added to show the indirect relationship. The connectivity map was generated from available published data (Ingenuity Systems). Each symbol for gene denotes the function of the interacting protein. Symbols representing specific categories of cellular molecules as well as interactive relationships are depicted in the legend. B, schematic representation of the SNVs identified in *MYH9*, *MYH10*, *MYH6*, and *RHOA*. Nucleotide-binding domains and protein domains are included. C, dual color FISH analysis of *MYH9* and *NF2* in MPM samples. Negative control (normal lymphoblast line with metaphases to confirm localization) is in the top left. The orange probe is specific for *NF2*, the green for *MYH9*.

"probably damaging" effect and one caused a reading frame shift. Twelve samples exhibited germline mutations in *MYH9*; seven had a predicted "possibly or probably damaging" effect. Although many mutations of *MYH9* have been identified in several other cancers, only R1576Q identified in our series has been previously described (24).

In 4 patients, tumor-specific mutations of ILK pathway–associated genes were identified: 3 in *MYH9* (1.4%; Q738*, K737N, A1197fs) and 2 in *RHOA* (1.4%; Y66N, A161V). One patient had in *MYH9* one germline and two tumor-specific mutations. No significant correlation was found between the mutations in the ILK pathway–associated genes and clinical or pathologic variables. No cell line exhibited mutations in these genes. Figure 1B depicts the mutations found in the myosin heavy chain genes and *RHOA*. Aberrations identified in *BAP1*, *NF2*, *TP53*, *MYH9*, *MYH6*, *MYH10*, *PIK3C2A*, *RHOA*, *TNFRSF1A*, 9p/*CDKN2A*, and 22q are illustrated in Supplementary Fig. S2.

Assessment of NF2 and MYH9 copy number status

Given the proximity of *NF2* and *MYH9* on the chromosome, 22q copy number status was explored. Although allelic loss in this region is common in MPM, the probes used for standard clinical FISH analysis do not distinguish copy number independently for these two genes. Dual-color FISH analysis using *MYH9*- and *NF2*-specific probes was undertaken for the 13 cases carrying *MYH9* mutation. Of the 13 primary tumors in which the two markers could be assessed, 2 (15%) exhibited no aberrations involving *NF2* or *MYH9*; 1 (8%) was abnormal by losing *NF2* only; 7 (54%) had loss of both markers; and 3 (23%) samples exhibited extra copies of both markers likely due to polyploidy

Table 3. Protein alteration and clinical information of the cases carrying *BAP1* and *TP53* germline mutations

Gene	Protein alteration	Functional classification	Gender	Other cancer (self)	Other cancer in the family
BAP1	W196*		Male	No	No
BAP1	W202C	Probably damaging (score 1)[a]	Male	No	Nasal (father), Breast (sister)
BAP1	V171*		Male	No	Renal and gastric (mother), lung (grandfather)
BAP1	G41S	Benign (score 0.078)[a]	Male	No	Lung (father)
BAP1	Splice site acceptor		Female	No	Prostate (father), Meningioma (mother), Bladder (sister)
TP53	R248W	Deleterious[b]	Female	No	Prostate (father), Rhabdomyosarcoma (grandmother)
TP53	D49N	Neutral[b]	Male	Skin cancer	No
TP53	C176F	Deleterious[b]	Female	Myelodysplasia, Acute myeloid leukemia	No
TP53	A86T	Neutral[b]	Male	No	Unknown (two sisters and grandparents)

[a]Polyphen (http://genetics.bwh.harvard.edu/pph2/).
[b]http://p53.iarc.fr/.

(Supplementary Table S5D; ref. 25). Two of the 7 cases displaying loss of both markers had tumor-specific mutation in both *MYH9* and *NF2*, whereas 5 had tumor-specific mutation of *MYH9* only. Furthermore, the case exhibiting *NF2* loss only presented two tumor-specific mutations in addition to one germline mutation in *MYH9*. Examples of FISH analysis are shown in Fig. 1C.

Mutual exclusivity

In MPM, tumor-specific mutations in *RHOA*, *MYH9* and *TP53* were mutually exclusive events that occurred more frequently in women (30%) than in men (12%) ($P = 0.023$). We examined the relationship between *RHOA* and *MYH9* in other cancers using the cBioPortal for Cancer Genomics (accessed July 13, 2015; ref. 24). Notably, in 26 of 31 (84%) tumor types that had mutations in both genes, *RHOA* and *MYH9* mutations had a strong tendency toward mutual exclusivity (Supplementary Table S6).

Analysis of TP53 in additional MPM cases

Given that mutations of *TP53* were found more commonly in women, and that women with MPM generally have lower levels of asbestos exposure than men, we expanded our validation cohort to power exploration of these associations. Mutational status of *TP53* was analyzed by Sanger sequencing in 136 additional MPM samples. Asbestos counts were available for 148 of 283 cases in the combined cohort, including tumors from 88 women and 67 patients with asbestos body counts in lung tissue consistent with background exposure ($\leq$ 50 fibers/g lung tissue; ref. 26). Thirty-eight of 283 patients (13%) had *TP53* point mutations, including 18 men (9%) and 20 women (23%), ($P = 0.004$; Supplementary Table S5B). Expanding the cohort added one case (total 4/283) with germline *TP53* mutation (R248W; Table 3). Although *TP53* mutations were found more frequently in tumors with background versus higher asbestos exposure, the analysis did not have sufficient power to exclude exposure level as a risk factor in either the whole cohort ($P = 0.068$) or among women ($P = 0.498$). No significant correlation of mutations in *TP53* was found to either survival, or histologic subtype.

Expression analysis of the candidate genes

A comparative exploratory analysis of MPM transcriptomic profiles was conducted to determine whether histologic subtype, survival, or gender are correlated with specific expression patterns in *BAP1*, *NF2*, *TP53*, *MYH9*, *MYH6*, *MYH10*, *PIK3C2A*, *RHOA*, *CDKN2A*, and *TNFRSF1A* (Supplementary Fig. S1; Supplementary Table S3). This cohort comprised 85 men and 66 women. Ten samples were also included in the sequencing analysis; these were pure epithelioid tumors showing no mutation in *BAP1*, *MYH9*, or *RHOA*.

Nonepithelioid (versus epithelioid) tumors expressed significantly higher levels of *BAP1* ($P < 0.001$), *MYH9* ($P < 0.001$), *RHOA* ($P < 0.001$), and *MYH10* ($P = 0.001$). *RHOA* was more highly expressed in men than women ($P = 0.001$). Expression levels of other genes examined were not correlated with gender or histology.

Patients with lower *BAP1* expression had improved overall survival ($P < 0.001$; Fig. 2A). The highest quartiles of *BAP1* expression were associated with twice the risk of death (HR = 2.31) compared with the lowest quartile, after adjusting for the independent effect of gender. The survival difference was similar across gender subgroups (male: HR = 2.20; $P = 0.005$; and female: HR = 2.38; $P = 0.004$; Fig. 2B). Similarly, the highest quartile of *MYH9* expression was associated with increased gender-adjusted risk of death (HR = 2.23) compared with the lower three quartiles ($P < 0.001$; Fig. 2C). MYH9 expression was associated with twice the risk of death in both males (HR = 2.26; $P = 0.001$) and females (HR = 2.17; $P = 0.022$; Fig. 2D). In the entire cohort, lower *RHOA* expression was associated with improved survival ($P < 0.001$; Fig. 2E). The highest quartile of *RHOA* expression was associated with twice the gender-adjusted risk of death (HR = 1.95) compared with the lower three quartiles. Analysis by gender subgroups showed that the highest quartile of *RHOA* expression was associated with increased risk of death (HR = 2.22; $P < 0.001$) compared with the lower three quartiles in males (Fig. 2F). No significant association was demonstrated between *RHOA* expression and the risk of death (HR = 1.42; $P = 0.385$) in females, possibly due to the relatively few females with tumor highly expressing RHOA (Fig. 2F). Survival analyses for *BAP1*, *MYH9*, and *RHOA* restricted to the epithelioid tumors showed similar conclusions. Expression levels of the other genes examined were not associated with survival either in the entire cohort or within gender subgroups.

Discussion

Realizing the potential of precision medicine requires identification of subgroups of patients deemed likely to respond to

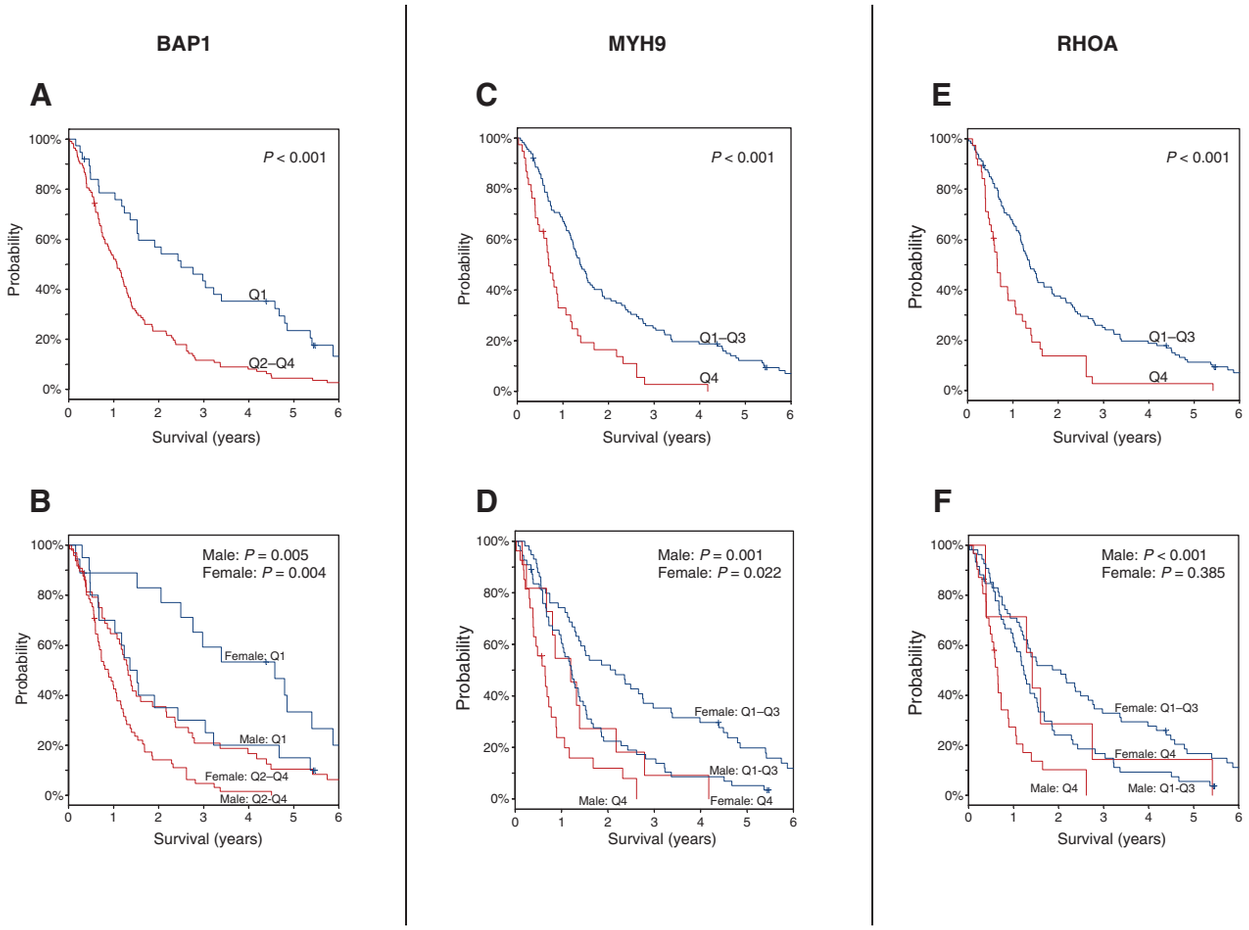

Figure 2.
Kaplan–Meier analysis of tumor-specific survival in patients with MPM according to *BAP1*, *MYH9*, and *RHOA* expression. Overall survival of 151 MPM patients grouped into quartiles (lowest Q1, Q2, Q3, Q4 highest) of *BAP1* (A and B), *MYH9* (C and D), and *RHOA* (E and F) transcriptomic profiles for all tumors (A, C, E) and by gender (B, D, F).

specific biologically based therapies. Such stratification only becomes possible as the genetic features that contribute to disease heterogeneity for a given tumor are elucidated (27).

Refinements of molecular subclassification based on comprehensive analysis of the genetic landscape are required to personalize treatment of MPM. Until recently, the genetics of MPM was primarily described in terms of deletions of specific chromosomal regions, particularly within 1p, 3p, 6q, 9p, 13q, 15q, and 22q (reviewed in ref. 28). *CDKN2A* and *NF2* are the tumor suppressor genes most commonly found mutated (8, 9, 29), and recently, evidence for a role for *BAP1* was demonstrated (10, 12). During the preparation of this work, a whole-exome sequencing study using DNA from 22 MPMs and matched blood samples found 517 somatic mutations across 490 mutated genes, confirmed frequent mutation in *BAP1*, *NF2*, and *CDKN2A*, and identified alterations of *CUL1* in 2 of 22 cases (30). However, the small number of patients analyzed neither allowed for clinical correlation, nor suggested a basis for patient stratification.

The current study validated candidate driver genes (*TP53*, *BAP1*, *NF2*, and *CDKN2A*) in large cohort of MPM cases. Although CUL1 was not sequenced among the validation cases, no CUL1 mutations were observed among the 10 whole-genome sequenced cases. Novel molecular alterations in *MYH9*, *MYH6*, *MYH10*, *PIK3C2A*, *RHOA*, and *TNFRSF1A* were documented, and bioinformatic analyses found these genes to be linked.

TP53 mutations occurred in 13% of MPM cases analyzed here. Mutations in this gene were more than twice as frequent in women than in men. In one prior study, *TP53* genotype was predictive of survival in women following adjuvant therapy for colon cancer (31). In another study of 152 *TP53* germline mutation carriers, *TP53* PIN3 polymorphism was found to have a sex-specific effect, conferring cancer risk in men ($P = 0.0041$) but not women (32). To our knowledge, this is the first report of *TP53* mutation in tumor and germline DNA in sporadic MPM or in patients with familial history of cancer. Interestingly, only germline mutations in women had predicted deleterious functional impact on p53, whereas the mutations identified in men had predicted neutral impact on the protein. No evidence was found in the clinical profile of patients carrying these *TP53* mutations to suggest Li-Fraumeni syndrome (33). Although women with MPM have *TP53* mutations at a higher rate compared with men, no significant correlation of *TP53* status was found to survival in this cohort.

A recent study reports BAP1 mutation in approximately 70% of MPM and suggests that large chromosomal deletions commonly inferred by immunohistochemistry are missed by Sanger sequencing (34). This may explain why *BAP1* was found mutated in 21% of the cases by targeted sequencing in the current study. Five cases showed germline *BAP1* mutations of which 4 had familial history of cancer. To date, *BAP1* germline mutations have been considered very rare in patients with sporadic MPM (35), and a recent study has shown that 23 MPM patients with *BAP1* germline mutations had an overall 7-fold increased long-term survival, independent of sex and age (36). In the current study, nonepithelioid MPM was associated with higher expression and less frequent mutation of *BAP1*. Furthermore, elevated *BAP1* expression was associated with twice the risk of death after adjusting for the independent effect of sex.

Several investigators have suggested that p16 protein expression may be predictive of favorable prognosis, and that down-regulation of p16 is significantly correlated with poor patient survival in various cancers (37, 38). In the current study, deletion of the p16 gene, *CDKN2A*, was correlated with shorter survival. *CDKN2A* deletions were more frequent in the nonepitheliod subtype among men. In contrast, 22q loss was more frequently associated with epithelioid subtype, but was not associated with survival.

In this study, 26 SNVs were identified in three myosin heavy chain genes (*MYH6*, *MYH9*, *MYH10*). Myosins are required for actin-based intracellular mobility and have been linked to cell proliferation, adhesion, and migration (39). The heavy chain, type A, myosin *MYH9* was the most commonly mutated in the current MPM cohort. This gene has been previously associated with cancer cell migration, invasion, and metastasis (40). In addition, it has been shown that the protein product, myosin IIA, is required for both stability and nuclear retention of p53 (40). Fifteen mutations of this gene were identified in 13 (9%) MPM patients, of which 6 had familial history of cancer. Three of the 15 mutations were tumor specific and 12 were germline. One patient carried two tumor specific and one germline mutation of *MYH9*.

Loss of *MYH9* alleles was also common. *MYH9* maps to 22q13.1 telomeric to the region where *NF2* is located (22q12.2). Loss of chromosome 22 is the single most consistent numerical cytogenetic change in MPM (9). It has been suggested that cancer genes other than *NF2* may be involved in some malignancies associated with chromosome 22 allelic losses, in which *NF2* mutations are not detected or found at very low frequencies (9). The probes used for clinical FISH analysis to detect 22q deletion hybridize to 22q11.2 (TUPL1) and 22q13 (ARSA). Because both *NF2* and *MYH9* are within this region, deletions encompassing both probes indicate loss of both genes. However, rearrangements associated with deletion of only one of the probes do not necessarily indicate deletion of either of these genes, and, conversely, cases lacking deletion of these probes could still have *NF2* and/or *MYH9* deletions. In the current study, dual-color FISH analysis using probe sets specific for each gene indicated that 45% of the samples with *MYH9* mutation and wild-type *NF2* had loss of one allele for both genes. This finding suggests that mutated *MYH9* may contribute to tumorigenesis in some 22q deletion cases.

RHOA encodes a Rho family GTPase, known to regulate the actin cytoskeleton in the formation of stress fibers and focal adhesions, as well as having a significant involvement in cancer signaling cascades (41–45). Two tumor-specific mutations have been identified in the validation cohort of this study. *RHOA* resides on 3p21.3 close to *BAP1* (3p21.1), another region frequently deleted in MPM.

The observations that *RHOA* signaling leading to *MYH9* activation in the processes of hemostasis and thrombosis (46), and the observed mutual exclusivity of *MYH9* and *RHOA* support the functional association of these two genes. The significance of *RHOA* and *MYH9* in MPM is supported by their association to clinical factors including gender, histology, and patient outcome after surgical therapy. The common relation of these and other genes found mutated in this study to the ILK pathway is intriguing. However, the role of the ILK pathway per se in MPM remains unclear.

In conclusion, the analysis of 10 genome pairs has highlighted novel molecular features in the molecular biology of MPM. The molecular events leading to MPM tumorigenesis appear complex, involving alterations in different genes in subgroups of patients. Chromosomal regions of common allelic loss may contain more than one gene involved in the transformation of a mesothelial cell. Some of the genetic abnormalities are associated with clinicopathologic variables such as histologic subtype, gender, and survival. Experience in other cancers suggests that studying much larger numbers of MPM genomes may be required for comprehensive molecular understanding of MPM.

Disclosure of Potential Conflicts of Interest

J.A. Fletcher reports receiving commercial research grant from AztraZeneca. J. Quackenbush has ownership interest (including patents) in GenoSpace, LLC. No potential conflicts of interest were disclosed by the other authors.

Authors' Contributions

Conception and design: A. De Rienzo, W.G. Richards, R. Bueno

Development of methodology: A. De Rienzo, N. Dao, A.C. Sideris, Y.E. Wang, P.S. Dal Cin, J.A. Fletcher, R. Rubio, S. Rudd, W.G. Richards

Acquisition of data (provided animals, acquired and managed patients, provided facilities, etc.): M.A. Archer, N. Dao, A.C. Sideris, Y. Zheng, Y.E. Wang, J.A. Fletcher, R. Rubio, K.J. Munir, J.R. Battilana, L.R. Chirieac, D.J. Sugarbaker, W.G. Richards, R. Bueno

Analysis and interpretation of data (e.g., statistical analysis, biostatistics, computational analysis): A. De Rienzo, M.A. Archer, B.Y. Yeap, A.C. Sideris, A.G. Holman, Y.E. Wang, J.A. Fletcher, L. Croft, J. Quackenbush, L.R. Chirieac, S.M. Ching, J. Wong, L.C. Tay, S. Rudd, R. Hercus, R. Bueno

Writing, review, and/or revision of the manuscript: A. De Rienzo, M.A. Archer, B.Y. Yeap, Y. Zheng, J.A. Fletcher, L. Croft, J. Quackenbush, D.J. Sugarbaker, W.G. Richards, R. Bueno

Administrative, technical, or material support (i.e., reporting or organizing data, constructing databases): M.A. Archer, B.Y. Yeap, D. Sciaranghella, L. Croft, P.E. Sugarbaker, J.R. Battilana, C. Gustafson, J. Wong, D.J. Sugarbaker, W.G. Richards

Study supervision: W.G. Richards, R. Bueno

Other (karyotype and FISh analysis in all samples investigated): P.S. Dal Cin

Disclaimer

The study sponsors played no role in the study design, collection, analysis, interpretation of data, writing of the report, or decision to submit the paper for publication.

Acknowledgments

We thank Julianne Barlow and Sarah C. Rogers for the technical support with the clinical information; the BWH CytoGenomics Core for technical assistance

in dual-color FISH analysis; Claire V. Meyerovitz and Michela E. Oster for technical support with data collection.

Grant Support

This work was supported by grants from the Mesothelioma Applied Research Foundation (A. De Rienzo), from the NCI (RO1CA120528 to R. Bueno), and the International Mesothelioma Program at Brigham and Women's Hospital.

The costs of publication of this article were defrayed in part by the payment of page charges. This article must therefore be hereby marked *advertisement* in accordance with 18 U.S.C. Section 1734 solely to indicate this fact.

Received March 17, 2015; revised August 11, 2015; accepted October 19, 2015; published OnlineFirst November 10, 2015.

References

1. Skammeritz E, Omland LH, Johansen JP, Omland O. Asbestos exposure and survival in malignant mesothelioma: a description of 122 consecutive cases at an occupational clinic. Int J Occup Environ Med 2011;2:224–36.
2. Henley SJ, Larson TC, Wu M, Antao VC, Lewis M, Pinheiro GA, et al. Mesothelioma incidence in 50 states and the District of Columbia, United States, 2003-2008. Int J Occup Environ Health 2013;19:1–10.
3. Vogelzang NJ, Rusthoven JJ, Symanowski J, Denham C, Kaukel E, Ruffie P, et al. Phase III study of pemetrexed in combination with cisplatin versus cisplatin alone in patients with malignant pleural mesothelioma. J Clin Oncol 2003;21:2636–44.
4. Travis WD, Brambilla E, Muller-Hermelink HK, Harris CC, eds. World Health Organization International Agency for Research on Cancer International Association for the Study of Lung Cancer International Academy of Pathology. Pathology and genetics of tumours of the lung, pleura, thymus and heart. Lyon, France: IARC Press, 2004.
5. Taioli E, Wolf AS, Camacho-Rivera M, Flores RM. Women with malignant pleural mesothelioma have a threefold better survival rate than men. Ann Thorac Surg 2014;98:1020–4.
6. Wolf AS, Richards WG, Tilleman TR, Chirieac L, Hurwitz S, Bueno R, et al. Characteristics of malignant pleural mesothelioma in women. Ann Thorac Surg 2010;90:949–56.
7. Stratton MR. Exploring the genomes of cancer cells: progress and promise. Science 2011;331:1553–8.
8. Carbone M, Kratzke RA, Testa JR. The pathogenesis of mesothelioma. Semin Oncol 2002;29:2–17.
9. Bianchi AB, Mitsunaga SI, Cheng JQ, Klein WM, Jhanwar SC, Seizinger B, et al. High frequency of inactivating mutations in the neurofibromatosis type 2 gene (NF2) in primary malignant mesotheliomas. Proc Natl Acad Sci U S A 1995;92:10854–8.
10. Bott M, Brevet M, Taylor BS, Shimizu S, Ito T, Wang L, et al. The nuclear deubiquitinase BAP1 is commonly inactivated by somatic mutations and 3p21.1 losses in malignant pleural mesothelioma. Nat Genet 2011;43:668–72.
11. de Assis LV, Locatelli J, Isoldi MC. The role of key genes and pathways involved in the tumorigenesis of Malignant Mesothelioma. Biochim Biophys Acta 2014;1845:232–47.
12. Testa JR, Cheung M, Pei J, Below JE, Tan Y, Sementino E, et al. Germline BAP1 mutations predispose to malignant mesothelioma. Nat Genet 2011;43:1022–5.
13. Ladanyi M, Zauderer MG, Krug LM, Ito T, McMillan R, Bott M, et al. New strategies in pleural mesothelioma: BAP1 and NF2 as novel targets for therapeutic development and risk assessment. Clin Cancer Res 2012;18:4485–90.
14. Yoshikawa Y, Sato A, Tsujimura T, Emi M, Morinaga T, Fukuoka K, et al. Frequent inactivation of the BAP1 gene in epithelioid-type malignant mesothelioma. Cancer Sci 2012;103:868–74.
15. Richards W, Van Oss S, Glickman J, Chirieac L, Yeap B, Dong L, et al. A microaliquoting technique for precise histological annotation and optimization of cell content in frozen tissue specimens. Biotech Histochem 2007:1–9.
16. Bueno R, De Rienzo A, Dong L, Gordon GJ, Hercus CF, Richards WG, et al. Second generation sequencing of the mesothelioma tumor genome. PLoS ONE 2010;5:e10612.
17. Drmanac R, Sparks AB, Callow MJ, Halpern AL, Burns NL, Kermani BG, et al. Human genome sequencing using unchained base reads on self-assembling DNA nanoarrays. Science 2010;327:78–81.
18. Li H, Durbin R. Fast and accurate short read alignment with Burrows-Wheeler transform. Bioinformatics 2009;25:1754–60.
19. McKenna A, Hanna M, Banks E, Sivachenko A, Cibulskis K, Kernytsky A, et al. The Genome Analysis Toolkit: a MapReduce framework for analyzing next-generation DNA sequencing data. Genome Res 2010;20:1297–303.
20. Cingolani P, Platts A, Wang le L, Coon M, Nguyen T, Wang L, et al. A program for annotating and predicting the effects of single nucleotide polymorphisms, SnpEff: SNPs in the genome of Drosophila melanogaster strain w1118; iso-2; iso-3. Fly 2012;6:80–92.
21. Shi L, Reid LH, Jones WD, Shippy R, Warrington JA, Baker SC, et al. The MicroArray Quality Control (MAQC) project shows inter- and intraplatform reproducibility of gene expression measurements. Nat Biotechnol 2006;24:1151–61.
22. Forbes SA, Bindal N, Bamford S, Cole C, Kok CY, Beare D, et al. COSMIC: mining complete cancer genomes in the Catalogue of Somatic Mutations in Cancer. Nucleic Acids Res 2011;39:D945–50.
23. Comabella M, Caminero AB, Malhotra S, Agullo L, Fernandez O, Reverter F, et al. TNFRSF1A polymorphisms rs1800693 and rs4149584 in patients with multiple sclerosis. Neurology 2013;80:2010–6.
24. Cerami E, Gao J, Dogrusoz U, Gross BE, Sumer SO, Aksoy BA, et al. The cBio cancer genomics portal: an open platform for exploring multidimensional cancer genomics data. Cancer Discov 2012;2:401–4.
25. Klorin G, Rozenblum E, Glebov O, Walker RL, Park Y, Meltzer PS, et al. Integrated high-resolution array CGH and SKY analysis of homozygous deletions and other genomic alterations present in malignant mesothelioma cell lines. Cancer Genet 2013;206:191–205.
26. Roggli VL, Sharma A, Butnor KJ, Sporn T, Vollmer RT. Malignant mesothelioma and occupational exposure to asbestos: a clinicopathological correlation of 1445 cases. Ultrastruct Pathol 2002;26:55–65.
27. Stevens EA, Rodriguez CP. Genomic medicine and targeted therapy for solid tumors. J Surg Oncol 2015;111:38–42.
28. De Rienzo A, Testa JR. Recent advances in the molecular analysis of human malignant mesothelioma. La Clinica Terapeutica 2000;151:433–8.
29. Ladanyi M. Implications of P16/CDKN2A deletion in pleural mesotheliomas. Lung Cancer 2005;49:S95–8.
30. Guo G, Chmielecki J, Goparaju C, Heguy A, Dolgalev I, Carbone M, et al. Whole-exome sequencing reveals frequent genetic alterations in BAP1, NF2, CDKN2A, and CUL1 in malignant pleural mesothelioma. Cancer Res 2015;75:264–9.
31. Warren RS, Atreya CE, Niedzwiecki D, Weinberg VK, Donner DB, Mayer RJ, et al. Association of TP53 mutational status and gender with survival after adjuvant treatment for stage III colon cancer: results of CALGB 89803. Clin Cancer Res 2013;19:5777–87.
32. Fang S, Krahe R, Bachinski LL, Zhang B, Amos CI, Strong LC. Sex-specific effect of the TP53 PIN3 polymorphism on cancer risk in a cohort study of TP53 germline mutation carriers. Hum Genet 2011;130:789–94.
33. Sorrell AD, Espenschied CR, Culver JO, Weitzel JN. Tumor protein p53 (TP53) testing and Li-Fraumeni syndrome: current status of clinical applications and future directions. Mol Diagn Ther 2013;17:31–47.
34. Nasu M, Emi M, Pastorino S, Tanji M, Powers A, Luk H, et al. High Incidence of Somatic BAP1 alterations in sporadic malignant mesothelioma. J Thorac Oncol 2015;10:565–76.
35. Betti M, Casalone E, Ferrante D, Romanelli A, Grosso F, Guarrera S, et al. Inference on germline BAP1 mutations and asbestos exposure from the analysis of familial and sporadic mesothelioma in a high-risk area. Genes Chromosomes Cancer 2015;54:51–62.

36. Baumann F, Flores E, Napolitano A, Kanodia S, Taioli E, Pass H, et al. Mesothelioma patients with germline BAP1 mutations have 7-fold improved long-term survival. Carcinogenesis 2014;36:76–81.
37. Huang K, Li LA, Meng YG, Fu XY. p16 expression in patients with cervical cancer and its prognostic significance: meta-analysis of published literature. Eur J Obstet Gynecol Reprod Biol 2014;183:64–9.
38. Singhal S, Vachani A, Antin-Ozerkis D, Kaiser LR, Albelda SM. Prognostic implications of cell cycle, apoptosis, and angiogenesis biomarkers in non-small cell lung cancer: a review. Clin Cancer Res 2005;11:3974–86.
39. Aguilar-Cuenca R, Juanes-Garcia A, Vicente-Manzanares M. Myosin II in mechanotransduction: master and commander of cell migration, morphogenesis, and cancer. Cell Mol Life Sci 2014;71:479–92.
40. Schramek D, Sendoel A, Segal JP, Beronja S, Heller E, Oristian D, et al. Direct *in vivo* RNAi screen unveils myosin IIa as a tumor suppressor of squamous cell carcinomas. Science 2014;343:309–13.
41. Cools J. RHOA mutations in peripheral T cell lymphoma. Nat Genet 2014;46:320–1.
42. Kakiuchi M, Nishizawa T, Ueda H, Gotoh K, Tanaka A, Hayashi A, et al. Recurrent gain-of-function mutations of RHOA in diffuse-type gastric carcinoma. Nat Genet 2014;46:583–7.
43. Palomero T, Couronne L, Khiabanian H, Kim MY, Ambesi-Impiombato A, Perez-Garcia A, et al. Recurrent mutations in epigenetic regulators, RHOA and FYN kinase in peripheral T cell lymphomas. Nat Genet 2014;46:166–70.
44. Sakata-Yanagimoto M, Enami T, Yoshida K, Shiraishi Y, Ishii R, Miyake Y, et al. Somatic RHOA mutation in angioimmunoblastic T cell lymphoma. Nat Genet 2014;46:171–5.
45. Yoo HY, Sung MK, Lee SH, Kim S, Lee H, Park S, et al. A recurrent inactivating mutation in RHOA GTPase in angioimmunoblastic T cell lymphoma. Nat Genet 2014;46:371–5.
46. Pleines I, Hagedorn I, Gupta S, May F, Chakarova L, van Hengel J, et al. Megakaryocyte-specific RhoA deficiency causes macrothrombocytopenia and defective platelet activation in hemostasis and thrombosis. Blood 2012;119:1054–63.